Helical Metallacyclophanes

DOI: 10.1002/anie.201306674

A Ball-Joint-Type Host–Guest System that Consists of Conglomerate Helical Metallacyclophanes**

*Haeri Lee, Tae Hwan Noh, and Ok-Sang Jung**

If suitable molecular units could be advantageously arranged, what would the resultant properties of their molecular aggregates be? This sort has inspired molecular engineers for the past decade.[1–7] The assembly and the related properties of novel supramolecular aggregates are a hot topic and, not entirely coincidentally, a great challenge in the field of molecular chemistry.[6–10] A full understanding of the driving forces behind those aggregations is a prerequisite for the design and construction of molecular arrays. Cyclophanes are attractive models for understanding weak transannular interactions as well as distinct π···π systems.[11–13] They can also serve as basic examples for explaining molecular recognition, chemosensing, molecular electronics, and electrical, magnetic, and capsule effects that are introduced by significant donor–acceptor and electron-transfer processes, or by through-space effects.[14–23] Metallacyclophanes have been synthesized by the coordination-directed self-assembly of metals and multidentate ligands.[14,24–29] These structures are of particular interest owing to the many and various advantages inherent to organic cyclophanes: easily accessible modularity for dimensions and topology,[14] and straightforward incorporation of functions, such as catalytic effects,[30,31] luminescence,[32] redox-activity,[33] electron transfer,[34] and helicity.[35,36] The elucidation of the thermodynamics and kinetics of such metallacyclophane systems would certainly provide important insights into the evolution and emergence of delicate supramolecular systems.[37,38] To that end, three important synthetic approaches have been introduced: angular directional bonding, symmetry interaction, and weak interaction.[16]

Helical motifs are ubiquitous in nature and have provided an important impetus for the generation of helical molecules. Indeed, discrete or polymeric helicates the synthesis of which is driven by coordination is intriguing, because it enables various applications, including asymmetric catalysis, chiral chemistry, nonlinear optical materials, template precursors, memory devices, biomimetics, DNA, structural biology, specific ion sensors, and molecular reaction vessels.[35,36,39–43] Helicity can be induced on purpose by means of conformational restrictions that are due to the coordination with metal ions.[42,43]

In this context, we employed a self-assembly approach that incorporates the three methods described above to construct racemic helical metallacyclophanes, (*P*,*M*)-$[Pd_3X_6(L^1)_2]$, by the reaction of $K_2[PdX_4]$ (X = Cl, Br) with the C_3-symmetric tridentate ligand L^1 as a programmed discrete helical component. A subsequent partial substitution reaction of (*P*,*M*)-$[Pd_3X_6(L^1)_2]$ with another C_3-symmetric tridentate ligand L^2, or direct self-assembly of $K_2[PdX_4]$ with both L^1 and L^2, produced unprecedented conglomerate crystals forming a ball-joint-type host–guest system, (*P*)-$[Pd_3X_6(L^1)_2]$@(*M*)-$[Pd_3X_6(L^1)(L^2)]$ and (*M*)-$[Pd_3X_6(L^1)_2]$@(*P*)-$[Pd_3X_6(L^1)(L^2)]$ (X = Cl, Br; L^1 = *N*,*N*′,*N*″-tris(2-pyridinylethyl)-1,3,5-benzenetricarboxamide;[44] L^2 = *N*,*N*′,*N*″-tris-(3-pyridinylpropyl)-1,3,5-benzenetricarboxylate; *P* = right-handed helix; *M* = left-handed helix). The synthesis of this host–guest system is an effective method for obtaining useful aggregates. Herein, we present a very effective strategy for the synthesis of such a system. Its crystal structures, the driving aggregative force behind it, and the reversible equilibrium between the aggregate and its dissociated species in solution are also discussed.

The self-assembly of $K_2[PdX_4]$ with L^1 at room temperature produced racemic crystalline products of helical trimetallacyclophanes, (*P*,*M*)-$[Pd_3X_6(L^1)_2]$ (X = Cl: (*P*,*M*)-**1**-Cl; X = Br: (*P*,*M*)-**1**-Br). Subsequent reaction of (*P*,*M*)-**1**-X with L^2 at 70 °C yielded unprecedented conglomerate crystals of chiral (*P*)-$[Pd_3X_6(L^1)_2]$@(*M*)-$[Pd_3X_6(L^1)(L^2)]$ (X = Cl: (*P*)-**1**-Cl@(*M*)-**2**-Cl; X = Br: (*P*)-**1**-Br@(*M*)-**2**-Br) and its enantiomeric (*M*)-$[Pd_3X_6(L^1)_2]$@(*P*)-$[Pd_3X_6(L^1)(L^2)]$ (X = Cl: (*M*)-**1**-Cl@(*P*)-**2**-Cl; X = Br: (*M*)-**1**-Br@(*P*)-**2**-Br; Scheme 1). At this temperature, a partial substitution reaction was achieved in *N*,*N*-dimethylformamide (DMF) or dimethyl sulfoxide (DMSO). A change in the molar ratio of the reactants did not have a significant effect on product formation in any case. Direct reaction of $K_2[PdX_4]$ with both L^1 and L^2 in appropriate molar ratios produced the same conglomerate crystals, even at room temperature. However, at room temperature, the second step of the two-step reaction does not occur, which indicates that the partial substitution reaction of (*P*,*M*)-**1**-X with L^2 requires slightly more vigorous conditions than the direct reaction. The crystalline solids are soluble in DMSO and DMF, but are almost insoluble in common organic solvents such as acetone, chloroform, and tetrahydrofuran. Recrystallizations of all of the products from DMF or DMSO yielded the same results irrespective of the co-solvent (acetone, EtOH, and MeOH), which indicates that all of the products were thermodynamically stable. The carbonyl stretching frequencies of (*P*,*M*)-**1**-Cl (1656 cm^{-1}) and (*P*,*M*)-

[*] H. Lee, T. H. Noh, Prof. Dr. O.-S. Jung
Department of Chemistry and
Chemistry Institute for Functional Materials
Pusan National University, Pusan 609-735 (Korea)
E-mail: oksjung@pusan.ac.kr

[**] This work was supported by a National Research Foundation of Korea (NRF) grant funded by the Korean Government (MEST; 2010-0026167 and 2011-0013576).

Supporting information for this article is available on the WWW under http://dx.doi.org/10.1002/anie.201306674.

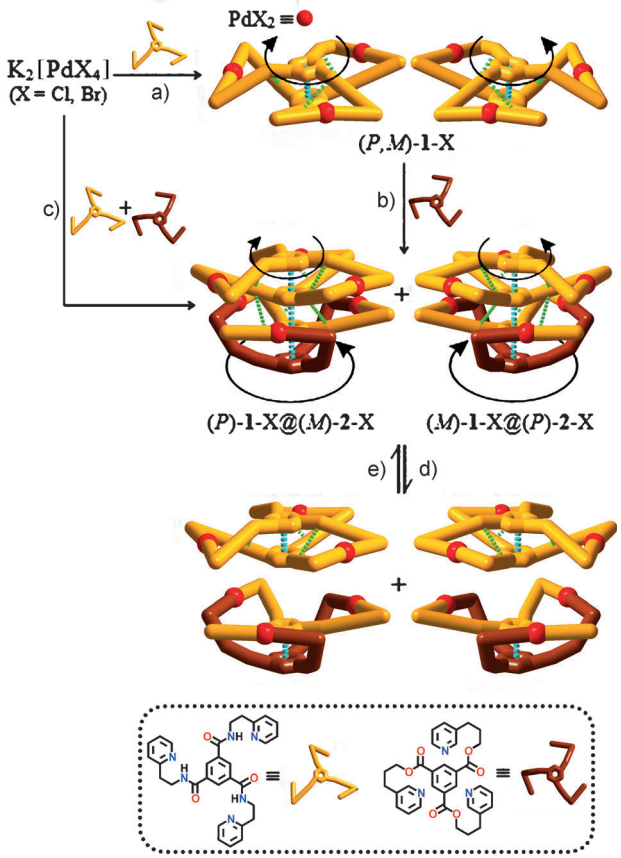

Scheme 1. Assembly process and solution behavior of ball-joint-type host–guest system consisting of conglomerate helical metallacyclophanes. Reaction conditions: a) racemic helical metallacyclophane mixture, (*P*,*M*)-**1**-X (X = Cl, Br), self-assembly in MeOH/DMF. b) conglomerate crystals of chiral (*P*)-**1**-Cl@(*M*)-**2**-Cl; the (*P*)-**1**-Br@(*M*)-**2**-Br aggregate and the enantiomeric (*M*)-**1**-Cl@(*P*)-**2**-Cl; the (*M*)-**1**-Br@(*P*)-**2**-Br aggregate, which was obtained by stirring in DMF at 70 °C for 5 h and addition of EtOH and Me_2CO, respectively, to the DMF solution. c) Direct reaction to obtain conglomerate crystals of chiral (*P*)-**1**-Cl@(*M*)-**2**-Cl; the (*P*)-**1**-Br@(*M*)-**2**-Br aggregate and the enantiomeric (*M*)-**1**-Cl@(*P*)-**2**-Cl; the (*M*)-**1**-Br@(*P*)-**2**-Br aggregate, which was obtained by stirring in DMF at 25–70 °C for 5 h and addition of EtOH and Me_2CO, respectively, to the DMF solution. d) High temperature or [D_7]DMF. e) Low temperature or [D_7]DMF and $CDCl_3$.

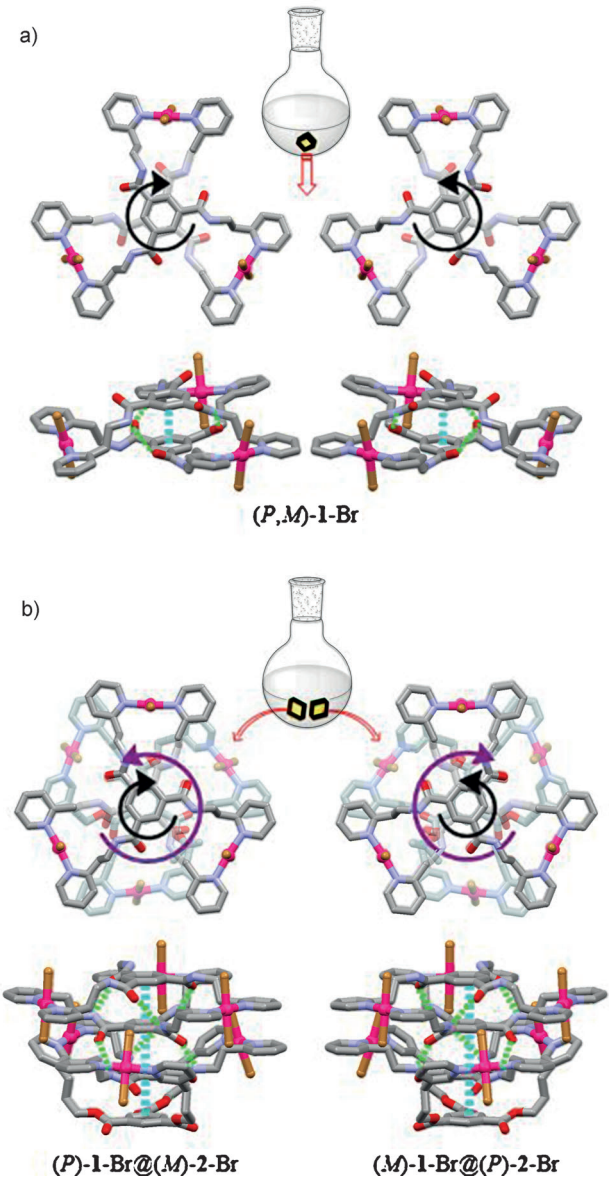

Figure 1. Top and side views of the crystal structures of (*P*,*M*)-**1**-Br (a) and its conglomerate crystals, (*P*)-**1**-Br@(*M*)-**2**-Br (b, left), and (*M*)-**1**-Br@(*P*)-**2**-Br (b, right).

1-Br (1656 cm^{-1}) showed a single band, whereas those of (*P*)-**1**-Cl@(*M*)-**2**-Cl/(*M*)-**1**-Cl@(*P*)-**2**-Cl (1716, 1652 cm^{-1}) and (*P*)-**1**-Br@(*M*)-**2**-Br/(*M*)-**1**-Br@(*P*)-**2**-Br (1722, 1650 cm^{-1}) exhibited two bands; these observations are consistent with the crystal structures.

X-ray analysis of single crystals of (*P*,*M*)-**1**-Cl and (*P*,*M*)-**1**-Br indicated that their skeletal structures consist of a C_3-symmetric trimetallacyclophane with a size of $24 \times 24 \times 9$ $Å^3$ (Figure 1; Supporting Information, Figure S1). In fact, except for the solvate molecules, the structure of (*P*,*M*)-**1**-Cl is very similar to that of (*P*,*M*)-**1**-Br. In particular, two tridentate L^1 ligands are connected to three PdX_2 moieties in a C_3-symmetric pinwheel fashion, which results in the formation of a racemic helical mixture of (*P*,*M*)-**1**-X. The local geometry around the palladium(II) center is approximately a typical square-planar arrangement in which the two nitrogen donors and the two chloride anions are arranged in a *trans* fashion (N-Pd-N = 177.3(2)° for (*P*,*M*)-**1**-Cl; N-Pd-N = 177.9(2)° for (*P*,*M*)-**1**-Br). The Pd···Pd distances in the equilateral triangles are 12.9597(6) Å for (*P*,*M*)-**1**-Cl and 13.0024(4) Å for (*P*,*M*)-**1**-Br. For the trimetallacyclophanes, a significant π···π interaction (3.431(3) Å for (*P*,*M*)-**1**-Cl; 3.435(3) Å for (*P*,*M*)-**1**-Br) exists between the two central and superimposable phenyl moieties (dihedral angle between the two phenyl moieties = 8.9(2)° for (*P*,*M*)-**1**-Cl; 8.6(2)° for (*P*,*M*)-**1**-Br). Three intramolecular NH···O=C hydrogen bonds (2.29 Å for (*P*,*M*)-**1**-Cl; 2.24 Å for (*P*,*M*)-**1**-Br) exist in the solid state. The *ab′ca′bc′* layers form along the *b* axis; the *a*, *b*, and *c* layers designate *P* helices, and *a′*, *b′*, and *c′* *M* helices (Supporting Information, Figure S2). Solvate molecules remain in the vacancies within the unit cell:

9 H_2O·3 MeOH for (*P*,*M*)-**1**-Cl and 6 H_2O·6 MeOH for (*P*,*M*)-**1**-Br. These methanol and water molecules evaporated at temperatures of 60–190 °C; the skeleton was stable up to 246 °C and 273 °C for (*P*,*M*)-**1**-Cl and (*P*,*M*)-**1**-Br, respectively (Supporting Information, Figure S3).

The conglomerate crystals of chiral (*P*)-**1**-Br@(*M*)-**2**-Br and its enantiomeric (*M*)-**1**-Br@(*P*)-**2**-Br were enantiomerically pure within the chiral space group, although the mixture of crystals is racemic (Figure 2). Except for the helicity, the crystal structures were the same. For (*P*)-**1**-Br@(*M*)-**2**-Br, the (*P*)-**1**-Br moiety is very similar to the structure of (*P*)-**1**-Br described above. The (*M*)-**2**-Br moiety, however, looks like a molecular bowl owing to the presence of the longer tridentate ligand L^2. The Pd···Pd distances in the equilateral triangles are 12.971(2) Å for the (*P*)-**1**-Br moiety, and 12.327(1) Å for the (*M*)-**2**-Br moiety. Both moieties still exhibit intramolecular π···π interactions at separations of 3.439(7) Å (dihedral angle between the two phenyl moieties = 3.3(4)°) and 3.351(7) Å (dihedral angle = 20.1(4)°), respectively. For chiral (*P*)-**1**-Br@(*M*)-**2**-Br, the two moieties of (*P*)-**1**-Br and (*M*)-**2**-Br are aggregated with different *P* and *M* helicities. The formation of a 300-atom aggregate of a size of 24 × 24 × 15 $Å^3$ can be attributed to one intermolecular π···π interaction (3.447(7) Å; dihedral angle between the two

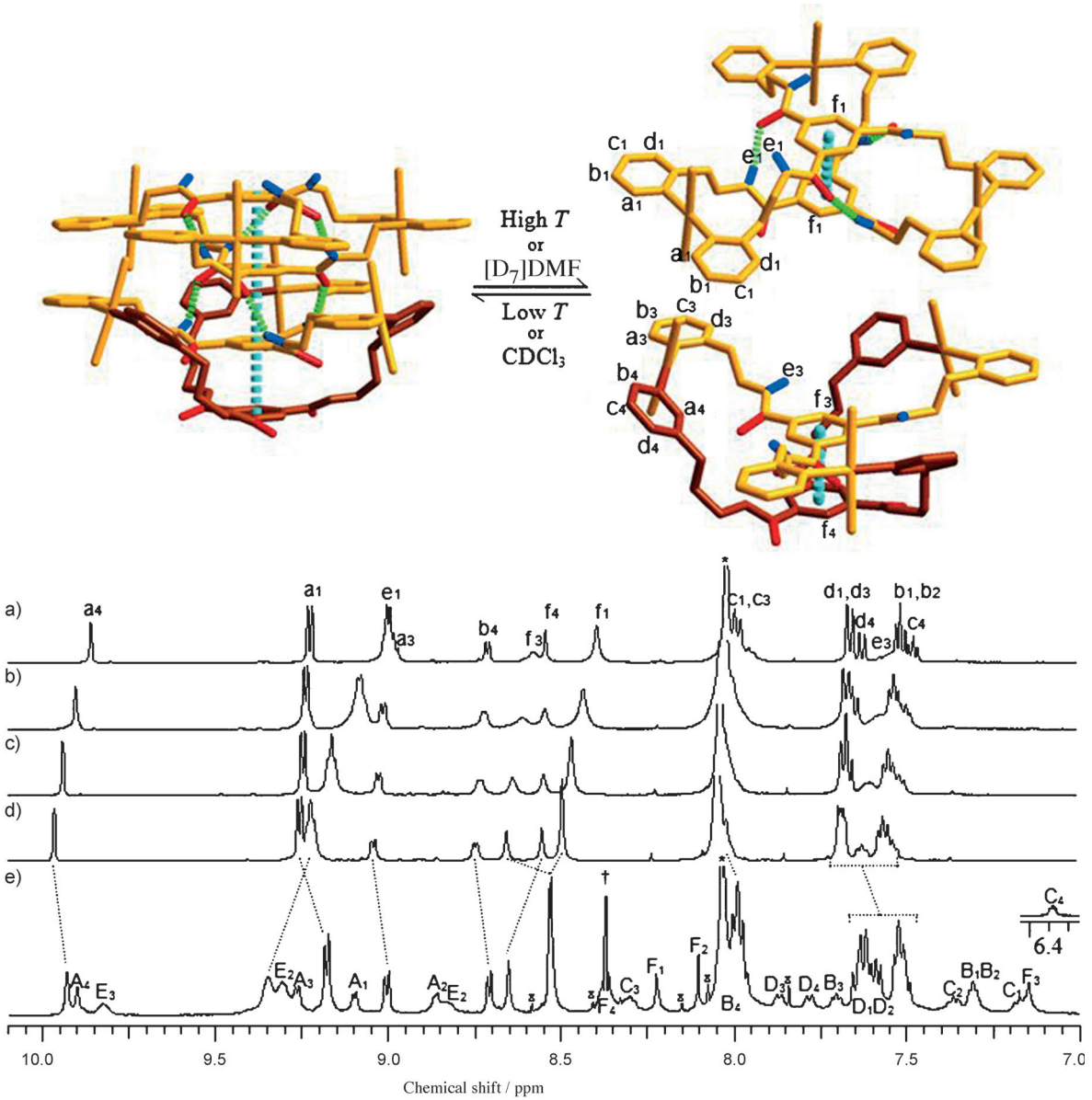

Figure 2. Partial ^{1}H NMR (500 MHz) spectra of (*P*)-[$Pd_3Br_6(L^1)_2$]@(*M*)-[$Pd_3Br_6(L^1)(L^2)$]/(*M*)-[$Pd_3Br_6(L^1)_2$]@(*P*)-[$Pd_3Br_6(L^1)(L^2)$] at 40 °C (a), 25 °C (b), 0 °C (c), and −30 °C (d) in [D_7]DMF, and at −30 °C (e) in mixture of [D_7]DMF and $CDCl_3$ (3:1). The ^{1}H NMR spectra reflect the temperature dependence ((a)–(d)) and solvent dependence (e) of the aggregate. (e) shows a very complex spectrum owing to the presence of seven sets of ligands, including L^1 and L^2, from three species in a mixture of [D_7]DMF and $CDCl_3$ (3:1). The capital letters and the lower-case letters (designated by dotted lines) denote the assignments of the aggregates and their dissociated species, respectively. Subscripts 1, 2, 3, and 4 designate the four ligands of the aggregate (up→bottom: 1, 2, 3, and 4; for the detailed assignments, see the Supporting Information, Figure S4). The 2D COSY spectrum of (b) and the full spectrum of (e) can be found in the Supporting Information, Figures S5 and S7, respectively.

phenyl moieties = 1.4(2)°), and three intermolecular NH···O=C hydrogen bonds (2.13 Å) between the two different helical moieties. Its enantiomer, (*M*)-**1**-Br@(*P*)-**2**-Br, has the same structure, except for its helicity. The crystal consists of *abcabc* layers. The solvate molecules, $6H_2O{\cdot}6$acetone, are found in the unit-cell vacancies, and evaporated at 50–190 °C. The skeleton of the aggregate is stable up to 276 °C. The crystal structures and the thermal stability of the (*P*)-**1**-Cl@(*M*)-**2**-Cl and (*M*)-**1**-Cl@(*P*)-**2**-Cl conglomerate crystals were identified in a similar fashion (Supporting Information, Figure S3).

Our strategy for the construction of the metallacyclophanes is shown in Figure 1. The question arises as to how such unique and discrete racemic trimetallacyclophanes, (*P*,*M*)-**1**-X, are so effectively formed. A combination of a square-planar palladium(II) center and the tridentate *o*-pyridyl ligand L^1 seems to be responsible for the pinwheel trimetallacyclophane. The length and the conformation of the tridentate *o*-pyridyl L^1 ligand are key tectonic elements for the self-assembly of the metallacyclophane system, as they induce a linear coordination to the palladium(II) center. Besides, the formation of the metallacyclophane system can be ascribed to the presence of intramolecular π···π interactions and three intramolecular NH···O=C hydrogen bonds. Furthermore, the formation of the metallacyclophanes was not significantly affected by changes in molar ratio, solvents or concentration; this result is consistent with the thermodynamic stability of the trimetallacyclophane. The helical motif can be induced by coordination of the C_3-symmetric tridentate in pinwheel fashion. We were also intrigued how the conglomerate crystal of the host–guest aggregate that consists of ten small components is constructed. It seems that the aggregate is formed by joint-ball-type interactions between the π···π interaction and the NH···O=C hydrogen bonds. The intermolecular π···π interaction (3.447(7) Å, dihedral angle = 1.4(4)°) and hydrogen bonds (NH···O=C = 2.13 Å; N···O=C = 2.86 Å) are very similar to those of graphite[45] and those of the cytosine–guanine pair in DNA,[46] respectively; they also are similar to the corresponding interactions in (*P*,*M*)-**1**-Cl or (*P*,*M*)-**1**-Br, which indicates that strong aggregation occurs in the solid state. Significantly, the combined different helicities afforded the conglomerate crystals in high yields for the first time. Furthermore, the combined intermolecular effects lead to the preferential formation of aggregates irrespective of the X anions, the molar ratio, concentration, or reaction procedure. The increase in π-electron density on the central phenyl group that is due to the presence of the amide and ester moieties can be partially attributed to the formation of strong aggregates. The present method that uses $K_2[PdX_4]$, L^1, and L^2 is the only means of constructing the unique conglomerate ball-joint-type aggregate. The position of the nitrogen donor and the spacer length of the tridentate ligand are key requirements for the formation of this structure. Indeed, none of the reactions of $K_2[PdX_4]$ with other *o*-, *m*-, or *p*-tridentate pyridyl ligands afforded analogous results.

To elucidate the behavior of the host–guest aggregates in solution, the temperature- and solvent-dependent ^{1}H NMR spectra of a racemic helical mixture of (*P*)-**1**-Br@(*M*)-**2**-Br/(*M*)-**1**-Br@(*P*)-**2**-Br were examined (Figure 2; Supporting Information, Figure S4), because (*P*)-**1**-Cl@(*M*)-**2**-Cl and (*M*)-**1**-Cl@(*P*)-**2**-Cl are marginally soluble in organic solvents, even in DMSO or DMF. The resonances for (*P*)-**1**-Br@(*M*)-**2**-Br and (*M*)-**1**-Br@(*P*)-**2**-Br in [D_7]DMF at room temperature could be assigned based on cross-peaks in the 2D COSY spectrum (Supporting Information, Figure S5). The ^{1}H NMR spectra indicated that the aggregates are fully dissociated in solution at room temperature, although the chemical shifts at e_1, f_1, f_3, and f_4 (Figure 2a) were shifted significantly downfield by the temperature decrease. These shifts indicated that the hydrogen bonds and the π···π interactions are, even in solution, significantly dependent on temperature (Figure 2a-2d). Therefore, sample cooling induces the dissociated species to approach each other even in solution. A very significant feature is the strong solvent dependence exhibited by the chemical shifts (Figure 2e): The addition of $CDCl_3$ to a [D_7]DMF solution (*v*/*v* = 1:3) at room temperature drastically changed the chemical shifts and led to peak broadening; this implies that the aggregate and its dissociated species were in equilibrium in solution. When the solution temperature was decreased, the band widths gradually sharpened (Supporting Information, Figure S6). Figure 2e and Figure S7 show the ^{1}H NMR spectrum in a $CDCl_3$/[D_7]DMF (1:3) solution at −30 °C; the resonances were assigned based on cross-peaks in the 2D COSY spectrum (Supporting Information, Figure S8). From this data, a strong dependence of the equilibrium, not on temperature but rather on solvent can be deduced. The host–guest aggregate exists as a mixture of the aggregate (*P*)-**1**-Br@(*M*)-**2**-Br/(*M*)-**1**-Br@(*P*)-**2**-Br and its dissociated species in a ratio of approximately 1:2. A very complex spectrum with seven sets of aromatic signals from the L^1 and L^2 moieties of the aggregate (A_1, A_2, A_3, A_4, etc.) and its dissociated species (a_1, a_3, a_4, etc.) is thus obtained. The ratio of the aggregate and the dissociated species should increase as the ratio of $CDCl_3$/[D_7]DMF increases, because the delicate equilibrium is highly sensitive to the solvation energy. However, in the present system, the $CDCl_3$/[D_7]DMF (1:3) solution is a solubility limitation; as expected, evaporation of the $CDCl_3$ solvent from the $CDCl_3$/[D_7]DMF solution effected a reversion to the spectrum originally recorded in [D_7]DMF.

The UV/Vis absorption spectra of (*P*,*M*)-**1**-Cl (394 nm) and (*P*)-**1**-Cl@(*M*)-**2**-Cl/(*M*)-**1**-Cl@(*P*)-**2**-Cl (389 nm), and of (*P*,*M*)-**1**-Br (419 nm) and (*P*)-**1**-Br@(*M*)-**2**-Br/(*M*)-**1**-Br@(*P*)-**2**-Br (414 nm) were measured in DMF (Supporting Information, Figure S9). (*P*)-**1**-Cl@(*M*)-**2**-Cl/(*M*)-**1**-Cl@(*P*)-**2**-Cl (389 nm) and (*P*)-**1**-Br@(*M*)-**2**-Br/(*M*)-**1**-Br@(*P*)-**2**-Br (414 nm) exhibited a 5 nm blue-shift relative to (*P*,*M*)-**1**-Cl (394 nm) and (*P*,*M*)-**1**-Br (419 nm), respectively, which suggests that π···π interactions are more effective in the aggregates than in the corresponding (*P*,*M*)-**1**-Cl and (*P*,*M*)-**1**-Br. The difference in wavelength between (*P*,*M*)-**1**-Cl (394 nm) and (*P*,*M*)-**1**-Br (419 nm) might arise from the fact that the introduction of heavier halogen atoms into metallacyclophane systems narrows the HOMO–LUMO band gap.[47]

In conclusion, the reaction of $K_2[PdX_4]$ with *N*,*N*′,*N*″-tris(2-pyridinylethyl)-1,3,5-benzenetricarboxamide (L^1) produces discrete C_3-symmetric racemic helical trimetallacyclo-

phanes, (*P*,*M*)-$[Pd_3X_6(L^1)_2]$. Subsequent reaction of (*P*,*M*)-$[Pd_3X_6(L^1)_2]$ with L^2 or direct reaction of $K_2[PdX_4]$ with L^1 and L^2 yields, via one π···π stacking and three NH···O=C hydrogen bonds as well as the combined helicity, a ball-joint-type aggregate consisting of unprecedented helical metallacyclophanes conglomerate crystals. In solution, the aggregate is in equilibrium with its dissociated species; this equilibrium is strongly solvent-dependent. This equilibrium is reminiscent of a "left and right" ball-and-socket-joint behavior. The remarkable formation of the unprecedented helical aggregate by coordination to metal ions can enhance our understanding of aggregation, including the relevant structural thermodynamics and stability. Further investigations of this system will help to realize applications of supramolecular host–guest systems, such as molecule-accommodating recognition, DNA binding, electronic transition, dynamic catalysis, and metal–graphene interactions.

Experimental Section

Preparation of (*P*,*M*)-$[Pd_3Br_6(L^1)_2]$: A methanol solution (10 mL) of *N*,*N*′,*N*″-tris(2-pyridinylethyl)-1,3,5-benzenetricarboxamide (L^1; 21 mg, 0.04 mmol) was slowly diffused into a DMF solution (5 mL) of $K_2[PdX_4]$ (30 mg, 0.06 mmol). Yellow crystals of (*P*,*M*)-$[Pd_3Br_6(L^1)_2]\cdot 6H_2O\cdot 6MeOH$ formed at the interface, and were obtained in a 69% yield (30 mg) after 5 days. m.p. = 273 °C (dec.); elemental analysis calcd (%) for $C_{60}H_{60}Br_6N_{12}O_6Pd_3\cdot 6H_2O\cdot 6CH_3OH$: C 36.97, H 4.51, N 7.84; found: C 37.10, H 4.50, N 7.90; ^{1}H NMR (500 MHz, [D$_7$]DMF): δ = 9.23 (d, J = 5.9 Hz, 3H), 9.08 (t, J = 5.4 Hz, 3H), 8.44 (s, 3H), 8.01 (dd, J = 6.0, 7.3 Hz, 3H), 7.67 (d, J = 7.3 Hz, 3H), 7.53 (dd, J = 5.9, 6.0 Hz, 3H), 4.35 (t, J = 7.8 Hz, 6H), 4.10 ppm (td, J = 5.4, 7.8 Hz, 6H); ^{13}C NMR (125 MHz, [D$_7$]DMF): δ = 166.53, 162.18, 153.89, 139.40, 135.08, 128.84, 126.31, 123.36, 40.02, 39.91 ppm; IR (KBr pellet): $\tilde{\nu}$ = 3484 (br), 3278 (br), 3070 (w), 2931 (w), 1656 (s), 1606 (m), 1548 (s), 1484 (m), 1440 (m), 1286 (m), 1097 (w), 1062 (w), 767 (m) cm^{-1}.

Preparation of (*P*)-$[Pd_3Br_6(L^1)_2]$@(*M*)-$[Pd_3Br_6(L^1)(L^2)]$/(*M*)-$[Pd_3Br_6(L^1)_2]$@(*P*)-$[Pd_3Br_6(L^1)(L^2)]$; Method 1: A DMF solution (5 mL) of (*P*,*M*)-$[Pd_3Br_6(L^1)_2]$ (128 mg, 0.06 mmol) and L^2 (9 mg, 0.015 mmol) was stirred at 70 °C for 5 h, acetone was then slowly diffused into this mixture. Yellow crystals of (*P*)-$[Pd_3Br_6(L^1)_2]$@(*M*)-$[Pd_3Br_6(L^1)(L^2)]\cdot 6H_2O\cdot 6Me_2CO$/(*M*)-$[Pd_3Br_6(L^1)_2]$@(*P*)-$[Pd_3Br_6(L^1)(L^2)]\cdot 6H_2O\cdot 6Me_2CO$ were obtained in a 64% yield (80 mg) after 5 days. Method 2: A mixture of L^1 (16 mg, 0.03 mmol) and L^2 (9 mg, 0.015 mmol) in DMF (2.5 mL) was slowly added to a DMF solution (2.5 mL) of $K_2[PdX_4]$ (30 mg, 0.06 mmol). The solution was stirred at 70 °C for 5 h and subsequently cooled to room temperature. Acetone was then slowly diffused into the DMF solution. Yellow crystals of (*P*)-$[Pd_3Br_6(L^1)_2]$@(*M*)-$[Pd_3Br_6(L^1)(L^2)]\cdot 6H_2O\cdot 6Me_2CO$/(*M*)-$[Pd_3Br_6(L^1)_2]$@(*P*)-$[Pd_3Br_6(L^1)(L^2)]\cdot 6H_2O\cdot 6Me_2CO$ were obtained in a 72% yield (90 mg) after 5 days. m.p. = 276 °C (dec.); elemental analysis calcd (%) for $C_{123}H_{123}Br_{12}N_{21}O_{15}Pd_6\cdot 6H_2O\cdot 6(CH_3)_2CO$: C 40.42, H 4.11, N 7.02; found: C 40.30, H 4.05, N 7.10; ^{1}H NMR (500 MHz, [D$_7$]DMF): δ = 9.90 (s, 3H), 9.23 (d, J = 5.9 Hz, 6H), 9.07 (br, 6H), 9.01 (d, J = 5.9 Hz, 3H), 8.72 (d, J = 4.9 Hz, 3H), 8.61 (s, 3H), 8.54 (s, 3H), 8.43 (s, 3H), 7.99 (dd, overlapped with solvent, 9H), 7.67 (d, J = 7.8 Hz, 9H), 7.64 (d, J = 7.8 Hz, 3H), 7.58 (br, 3H), 7.53(dd, J=5.9, 7.8 Hz, 9H), 7.49 (dd, J = 5.9, 7.8 Hz, 3H), 4.44 (t, J = 5.9 Hz, 6H), 4.34 (br, 18H), 4.23 (br, 6H), 4.09 (br, 12H), 3.10 (t, J = 5.9 Hz, 6H), 2.35 ppm (br, 6H); ^{13}C NMR (150 MHz, [D$_7$]DMF; see Figure S10 for the spectrum): δ = 166.59, 166.00, 164.79, 161.70, 155.43, 153.86, 153.82, 151.55, 148.93, 148.87, 143.86, 139.39, 139.34, 139.25, 139.02, 135.12, 133.83, 131.23, 129.07, 128.86, 127.16, 126.34, 125.33, 123.38, 64.71, 40.82, 40.21, 40.01, 39.90 ppm; IR (KBr pellet): $\tilde{\nu}$ = 3535 (br), 3351 (br), 3068 (w), 2952 (w), 1722 (m), 1650 (s), 1606 (m), 1540 (s), 1484 (m), 1436 (m), 1290 (m), 1245 (m), 769 (m) cm^{-1}.

X-ray crystal-structure determination: CCDC 951935 ((*P*,*M*)-**1**-Cl·9H$_2$O·3MeOH), 951936 ((*P*,*M*)-**1**-Br·6H$_2$O·6MeOH), 951937 ((*P*)-**1**-Cl@(*M*)-**2**-Cl), 951938 ((*M*)-**1**-Cl@(*P*)-**2**-Cl), 951939 ((*P*)-**1**-Br@(*M*)-**2**-Br·6H$_2$O·6Me$_2$CO), and 951940 ((*M*)-**1**-Br@(*P*)-**2**-Br·6H$_2$O·6Me$_2$CO) contain the supplementary crystallographic data for this paper. These data can be obtained free of charge from The Cambridge Crystallographic Data Centre via www.ccdc.cam.ac.uk/data_request/cif.

Received: July 31, 2013
Published online: September 20, 2013

Keywords: cyclophanes · helical conglomerates · host–guest systems · π interactions · supramolecular chemistry

[1] S. A. Bourne, J. Lu, A. Mondal, B. Moulton, M. J. Zaworotko, *Angew. Chem.* **2001**, *113*, 2169 – 2171; *Angew. Chem. Int. Ed.* **2001**, *40*, 2111 – 2113.
[2] V. Percec, M. Peterca, M. J. Sienkowska, M. A. Ilies, E. Aqad, J. Smidrkal, P. A. Heiney, *J. Am. Chem. Soc.* **2006**, *128*, 3324 – 3334.
[3] G. Zhang, G. Yang, N. Wu, J. S. Ma, *Cryst. Growth Des.* **2006**, *6*, 229 – 234.
[4] J. L. Atwood, *Nat. Mater.* **2002**, *1*, 91 – 92.
[5] Y. Ke, L. L. Ong, W. M. Shih, P. Yin, *Science* **2012**, *338*, 1177 – 1183.
[6] H. Abourahma, B. Moulton, V. Kravtsov, M. J. Zaworotko, *J. Am. Chem. Soc.* **2002**, *124*, 9990 – 9991.
[7] K. Tahara, S. Okuhata, J. Adisoejoso, S. Lei, T. Fujita, S. D. Feyter, Y. Tobe, *J. Am. Chem. Soc.* **2009**, *131*, 17583 – 17590.
[8] J. Lu, A. Mondal, B. Moulton, M. J. Zaworotko, *Angew. Chem.* **2001**, *113*, 2171 – 2174; *Angew. Chem. Int. Ed.* **2001**, *40*, 2113 – 2116.
[9] S. Schlickum et al., *J. Am. Chem. Soc.* **2008**, *130*, 11778-11782; see the Supporting Information.
[10] B. I. Park, I. S. Chun, Y.-A. Lee, K.-M. Park, O.-S. Jung, *Inorg. Chem.* **2006**, *45*, 4310 – 4312.
[11] R. Gleiter, D. Kratz, *Acc. Chem. Res.* **1993**, *26*, 311 – 318.
[12] R. Gleiter, B. Hellbach, S. Gath, R. J. Schaller, *Pure Appl. Chem.* **2006**, *78*, 699 – 706.
[13] M. Shibahara, M. Watanabe, T. Iwanaga, K. Ideta, T. Shinmyozu, *J. Org. Chem.* **2007**, *72*, 2865 – 2877.
[14] R. Lin, J. H. K. Yip, K. Zhang, L. L. Koh, K.-Y. Wong, K. P. Ho, *J. Am. Chem. Soc.* **2004**, *126*, 15852 – 15869.
[15] T. Kawase, H. Kurata, *Chem. Rev.* **2006**, *106*, 5250 – 5273.
[16] F.-B. Su, Q.-S. Li, X.-S. Zeng, X.-B. Leng, Z.-Z. Zhang, *Organometallics* **2004**, *23*, 632 – 634.
[17] S. Leininger, B. Olenyuk, P. J. Stang, *Chem. Rev.* **2000**, *100*, 853 – 908.
[18] M. Shibahara, M. Watanabe, T. Iwanaga, T. Matsumoto, K. Ideta, T. Shinmyozu, *J. Org. Chem.* **2008**, *73*, 4433 – 4442.
[19] M. Castellano, F. R. Fortea-Per'ez, S.-E. Stiriba, M. Julve, F. Lloret, D. Armentano, G. De Munno, R. Ruiz-Garciá, J. Cano, *Inorg. Chem.* **2011**, *50*, 11279 – 11281.
[20] S. O. Kang, V. W. Day, K. Bowman-James, *Org. Lett.* **2008**, *10*, 2677 – 2680.
[21] K. A. Doris, D. E. Ellis, M. A. Ratner, T. J. Marks, *J. Am. Chem. Soc.* **1984**, *106*, 2491 – 2497.
[22] T. H. Noh, E. J. Heo, K. H. Park, O.-S. Jung, *J. Am. Chem. Soc.* **2011**, *133*, 1236 – 1239.
[23] Y. Yamauchi, M. Fujita, *Chem. Commun.* **2010**, *46*, 5897 – 5899.
[24] S. R. Seidel, P. J. Stang, *Acc. Chem. Res.* **2002**, *35*, 972 – 983.
[25] B. J. Holliday, C. A. Mirkin, *Angew. Chem.* **2001**, *113*, 2076 – 2097; *Angew. Chem. Int. Ed.* **2001**, *40*, 2022 – 2043.

[26] G. F. Swiegers, T. J. Malefetse, *Coord. Chem. Rev.* **2002**, *225*, 91 – 121.
[27] F. A. Cotton, C. Lin, C. A. Murillo, *Acc. Chem. Res.* **2001**, *34*, 759 – 771.
[28] J. Hua, W. Lin, *Org. Lett.* **2003**, *5*, 2765 – 2768.
[29] M.-C. Dul et al., *Inorg. Chem.* **2010**, *49*, 11264-11266; see the Supporting Information.
[30] S. J. Lee, A. Hu, W. Lin, *J. Am. Chem. Soc.* **2002**, *124*, 12948 – 12949.
[31] N. C. Gianneschi, P. A. Bertin, S. T. Nguyen, C. A. Mirkin, L. N. Zakharov, A. L. Rheingold, *J. Am. Chem. Soc.* **2003**, *125*, 10508 – 10509.
[32] S.-S. Sun, J. A. Anspach, A. J. Lees, P. Y. Zavalij, *Organometallics* **2002**, *21*, 685 – 693.
[33] K. E. Splan, M. H. Keefew, A. M. Massari, K. A. Walters, J. T. Hupp, *Inorg. Chem.* **2002**, *41*, 619 – 621.
[34] M. Castellano, R. Ruiz-Garcia, J. Cano, M. Julve, F. Lloret, Y. Journaux, G. De Munnod, D. Armentano, *Chem. Commun.* **2013**, *49*, 3534 – 3536.
[35] H. Miyake, H. Tsukube, *Supramol. Chem.* **2005**, *17*, 53 – 59.
[36] E. C. Constable, *Chem. Soc. Rev.* **2013**, *42*, 1637 – 1651.
[37] A. V. Davis, R. M. Yeh, K. N. Raymond, *Proc. Natl. Acad. Sci. USA* **2002**, *99*, 4793 – 4796.
[38] M. J. Levin, P. J. Stang, *J. Am. Chem. Soc.* **2000**, *122*, 7428 – 7429.
[39] M. Albrecht, *Chem. Rev.* **2001**, *101*, 3457 – 3497.
[40] J. D. Watson, F. H. C. Crick, *Nature* **1953**, *171*, 737 – 738.
[41] J. H. Jung, Y. Ono, S. Shinkai, *Chem. Eur. J.* **2000**, *6*, 4552 – 4557.
[42] O.-S. Jung, Y. J. Kim, Y.-A. Lee, J. K. Park, H. K. Chae, *J. Am. Chem. Soc.* **2000**, *122*, 9921 – 9925.
[43] K. H. Park, T. H. Noh, Y.-B. Shim, O.-S. Jung, *Chem. Commun.* **2013**, *49*, 4000 – 4002.
[44] H. Lee, T. H. Noh, O.-S. Jung, *CrystEngComm* **2013**, *15*, 1832 – 1835.
[45] P. Delhaes in *The World of Carbon: Graphite and Precursors*, Gordon and Breach, New York, **2001**.
[46] C. Fonseca Guerra, F. M. Bickelhaupt, *Angew. Chem.* **1999**, *111*, 3120 – 3122; *Angew. Chem. Int. Ed.* **1999**, *38*, 2942 – 2945.
[47] K. Kobayashi, H. Masu, A. Shuto, K. Yamaguchi, *Chem. Mater.* **2005**, *17*, 6666 – 6673.

